J. Fluid Mech. (1966), *vol.* 24, *part* 4, *pp.* 769–779
Printed in Great Britain

Boundary dissipation of oscillatory waves

By W. G. VAN DORN
Scripps Institution of Oceanography, University of California, San Diego

(Received 14 April 1965 and in revised form 17 September 1965)

The attenuation of progressive, dispersive, oscillatory wave systems by dissipation within the viscous boundary layer in a long laboratory channel was studied both experimentally and theoretically, for the conditions of uniform water depth and over uniform impermeable slopes. In general, the observed dissipation exceeded that predicted by linear, small-amplitude theory for the boundary layer on the sides and bottom of the channel. On the hypothesis that the additional dissipation might be due to the presence of a similar boundary layer at the free water surface, the theory is extended to include the surface effect. The experimental results essentially confirm the theory—even in the markedly nonlinear region near shore.

1. Introduction

Many experimenters have reported that the observed attenuation coefficients for oscillatory waves propagating in a rectangular channel appear to be substantially greater than can be explained by viscous damping within the boundary layers on the sides and bottoms of their channels. In a recent review, Hunt (1963) remarks: 'The attenuation predicted by linear theory does not appear ever to have been verified with much accuracy, although when correctly applied the error is not as much as the 35 % quoted by Grosch (1962).' An alternative, but unconvincing, attempt to explain the excess dissipation by assuming shear separation and a quadratic velocity distribution within the boundary layer was proposed by Eagleson (1959). A similar effect was observed by the author during an experimental investigation of the reflexion of dispersive, oscillatory wave systems from sloping beaches, where it was found necessary (because of the small scale of the experiment) to account mathematically for the viscous attenuation in order to explain the observed enhancement in shoaling water. In these experiments it was found that while the observed attenuation agreed with that computed for the solid boundaries when the water was fresh, the former tended to increase with time to some higher limiting value, usually within an hour.

Surprisingly, no one seems to have suggested that this discrepancy might arise through neglect of dissipation at the free surface, because of a contaminating surface film almost invariably present unless the surface is specially prepared, although Keulegan (1959) found reasonably good agreement with the linear theory for standing waves when the surface was kept clean. The theory of dissipation of deep water waves by contaminating surface films is discussed briefly by Lamb (1945) and in considerable detail by Dorrestein (1951), and has

been beautifully confirmed by the experimental investigations of Davies & Vose (1965). Physically, wave supression by films is due to the variations of surface tension caused by extensions and contractions of the contaminated surface.

Mathematically, the total viscous dissipation for plane, monochromatic waves propagating over a distance x in deep water can be expressed in terms of a damping coefficient Δ by

$$\eta = \eta_0 e^{-\Delta x}, \tag{1}$$

where η and η_0 are the initial and final wave amplitudes, respectively. At constant frequency ω, Δ increases with increasing surface contamination from its initial value for a clean (mobile) surface, $\Delta_m = 8\nu k^2/U$, to a limiting value for a fully contaminated (immobile) surface,

$$\Delta_{imm} = (k/2U)(\nu\omega/2)^{\frac{1}{2}}, \tag{2}$$

where $k = 2\pi/\lambda$ is the wave-number, ν is the kinematic viscosity, and U is the wave group velocity. The transition $\Delta_m \to \Delta_{imm}$ depends quite intimately upon the surface chemistry of the contaminating agent and, under certain conditions, may pass through an intervening maximum. However, if, as in the following, we confine ourselves to frequencies lower than about 3 cycles/sec†, the transition is smooth and, as shown below, appears to reach completion even at the small concentrations of contaminants usually present in ordinary tap water. The end state $\Delta = \Delta_{imm}$ is characterized by annulment of the horizontal component of wave velocity at the surface while, for oscillations of small amplitude ($\eta \ll \lambda$), the vertical component of the motion is essentially unaffected by the film.

In the present paper an expression is obtained for the surface-film effect on gravity waves in water of finite depth, under the assumption that the surface is fully contaminated (immobile). It is shown that this effect, when combined with the attenuation predicted for a viscous laminar layer on the boundaries of the wave channel, suffices to explain the observed total dissipation, except in the cases where special measures were taken to prevent surface contamination. Because the surface dissipation may often be larger than that on the boundaries under experimental conditions common to wave model studies, and also because it is almost impossible to maintain a clean surface under ordinary laboratory conditions, it is suggested that model results may often be seriously in error unless the former is taken into account.

2. Viscous dissipation in a rectangular channel

In a channel of uniform width b and depth h the damping coefficient Δ_b due to boundary dissipation of periodic gravity waves has been given by Hunt (1952) as

$$\Delta_b = \frac{2k}{b}\left(\frac{\nu}{2\omega}\right)^{\frac{1}{2}} \frac{kb + \sinh 2kh}{2kh + \sinh 2kh}. \tag{3}$$

† Equation (2) involves the surface tension implicitly in so far as it affects the group velocity. This effect also becomes negligible at low frequencies.

Under the same conditions, and assuming the free surface to be horizontally immobilized, the surface damping coefficient Δ_s can be expressed in similar form as (Appendix 1)

$$\Delta_s = \frac{2k}{b}\left(\frac{\nu}{2\omega}\right)^{\frac{1}{2}} \frac{kb\sinh^2 kh}{2kh+\sinh 2kh}. \tag{4}$$

When, as in the present experiments, the wave train is dispersive, having been generated by a single impulsive disturbance, the damping can still be computed by (3) and (4) provided only that each frequency is referred to its appropriate spectral amplitude $\eta[\omega(x,t)]$, as defined by the envelope of the wave train. With dispersion, however, there is an additional amplitude decay due to frequency separation (Kranzer & Keller 1959)

$$(\eta/\eta_0)_\omega \sim (x/x_0)^{-\frac{1}{2}}. \tag{5}$$

Combining (1), (3), (4) and (5), the total amplitude change at constant frequency after travelling a distance $x-x_0$ is

$$\begin{aligned}(\eta/\eta_0)_\omega &= (x/x_0)^{-\frac{1}{2}}\exp\left[-(\Delta_b+\Delta_s)(x-x_0)\right] \\ &= \left(\frac{x}{x_0}\right)^{-\frac{1}{2}}\exp\left[-\frac{2k(x-x_0)}{b}\left(\frac{\nu}{2\omega}\right)^{\frac{1}{2}}\left(\frac{bk\cosh^2 kh+\sinh 2kh}{2kh+\sinh 2kh}\right)\right].\end{aligned} \tag{6}$$

Hunt (1952) has also given an expression for the change in amplitude of periodic waves in a channel where the bottom slopes uniformly $[h = h_0 - s(x-x_0)]$. Upon correcting an error of integration in his final result, adding a term for the surface dissipation, and modifying the exponential coefficient to take account of dispersion as well as shoaling enhancement,† one obtains (Appendix 2)

$$(\eta/\eta_0)_\omega = \left[\frac{n\beta_0 U_0}{U}\right]^{\frac{1}{2}}\left[\sum_0^m \beta\right]^{-\frac{1}{2}}\exp\left\{\frac{1}{s}\left(\frac{\nu}{2\omega}\right)^{\frac{1}{2}}\left[\left(\frac{2}{b}+\frac{\omega^2}{g}\right)(kh-k_0h_0)-\tfrac{1}{2}(k-k_0)\right]\right\}, \tag{7}$$

where $\beta = -\partial(1/U^2)/\partial k$ and the subscript 0 indicates that a quantity is to be evaluated at $h = h_0$. In (7) n and m refer to the number of small, equal increments δx along the channel from the point of wave generation to the foot of the slope ($x = x_0$) and any point $x > x_0$ on the slope where the depth is $h(x)$, respectively.

In addition to the assumptions already made, that the surface be horizontally immobile and that the frequency be low enough so that the wave-number (and group velocity) are independent of surface tension, equations (6) and (7) also assume that the inviscid potential flow obtains everywhere in the region interior to the viscous boundary layers, whose thickness is given approximately by $(\nu/\omega)^{\frac{1}{2}}$; the wave motion itself is assumed to be given by small-amplitude, linear theory. Lastly, in the derivation of the shoaling coefficient it is assumed that no reflexions occur from the sloping beach and that the local group velocity is everywhere the same as if the water depth were uniform and equal to the local depth.

† The behaviour of a dispersive wave train in water of variable depth has been discussed previously (Van Dorn 1964).

The additional assumptions require, essentially, that the following inequalities be satisfied:

$$(1)\ \text{Linearity},\ \eta/k^2h^3 \ll 1;\quad (2)\ \text{small amplitude},\ \eta/h \ll 1;$$
$$(3)\ \text{geometric optics},\ s/kh \ll 1.$$

A discussion of the validity of these assumptions in the present experiments is given in §6.

3. Experimental facilities

The wave dissipation experiments were carried out in a rectangular plywood channel of width $b = 41{\cdot}3$ cm, depth $h_{\max} = 38$ cm, and length $l = 27$ m. The plywood had a phenolic plastic coating that was fine-sanded with emery cloth for additional smoothness. The channel was reinforced by external steel bracing

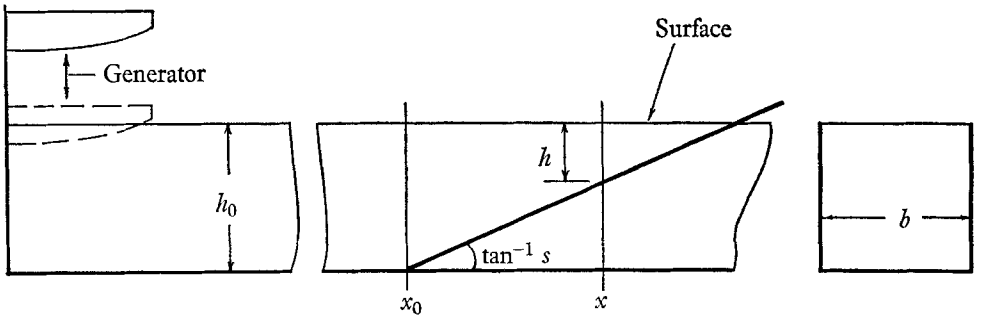

FIGURE 1. Diagram of wave channel showing parabolic wave generator.

at 60 cm intervals to insure a tolerance of less than $\pm 0{\cdot}5$ mm throughout its length, and the structure was carefully levelled and bolted to the concrete floor. Removable lid sections were provided to reduce evaporation and exclude dust. The channel was also equipped with a small swimming-pool filter, circulating pump, and surface skimmer.

Dispersive wave trains were generated at one end of the channel by a vertical single-stroke, impulsive generator bar having a parabolic cross-section (figure 1). The generator moved in heavy guides divorced from the channel structure, and was driven through a rocking beam and bell-crank by a variable-speed motor. The motor had a magnetic clutch-brake and a travel-limit cam, such that the generator could be started from top-centre, complete one down-and-up stroke, and be stopped in its initial position by automatic sequencing of the clutch and brake. Generator immersion was variable, but occurred during only a small fraction of the stroke. Because the stroke length, motor speed, immersion depth, and generator dimensions were all adjustable, a wide variety of wave envelope shapes could be produced.

Beaches of arbitrary slope were made up from heavy plate glass supported on aluminium bars that were wedged between the channel sides by expansion bolts. The glass plates were bevelled along both edges and sealed to the walls by continuous neoprene O-ring stock, in order to prevent wave energy from 'leaking' into the region behind the beaches.

Wave amplitudes were measured at arbitrary intervals along the channel by electrical strain-gauge pressure transducers suspended above the water from movable structures standing alongside the channel. Each transducer was equipped with a probe of copper capillary tubing 2 cm long and 1 mm diameter which penetrated the surface vertically to a depth of 1 cm. Wave signals were cabled to a central recording station, amplified, and recorded on a Minneapolis Honeywell galvanometer strip-chart recorder. The transducers were calibrated statically against a high-precision capacitance gauge, and dynamically by motion-pictures taken through a magnifying optical reticule profilometer set in the channel wall so as to intersect the still water surface. The reproducible measurement accuracy was found to be better than 0·001 cm at all frequencies considered ($\pi \leqslant \omega \leqslant 5\pi$). With such high resolution, wave amplitudes were limited to $\pm$ 5 mm and one's heartbeat was plainly visible on the recorder when standing on the concrete beside the channel. Even an automobile passing on the roadway 100 yd. away produced large spurious vibrations, requiring repetition of any experiments then under way.

4. Experimental procedure

Because the surface-tension effect appeared to increase with time after the renewal of water in the channel, the first experiments were aimed towards exploring its rate of increase. The tank was scrubbed, rinsed, and refilled with fresh (tap) water to a depth of 30 cm. Transducers were installed at distances of 4 and 8 m from the generator, and wave trains generated under identical conditions were recorded at successive intervals of 20 min. It was found that the wave amplitudes measured at equal times following the generation pulse progressively diminished for about an hour, following which no further diminution was observed. This latter condition was presumed to represent the establishment of some sort of contaminating film on the water surface. It was remarkable that the fully contaminated surfaces exhibited no obviously visible manifestation, the water always appearing to be in every respect as clear and fresh as when uncontaminated. After several hours, a temporary return to the uncontaminated condition could be brought about by filtering and skimming the water. These experiments were repeated, using distilled water in the channel, resulting in deferment of the fully contaminated condition by as long as 24 h, but the cost of daily renewal of 1000 gal. of fresh water could not be justified for the remaining experiments. Thereafter, all tests were run with tap water which had been left standing for an hour or more.

Dissipation experiments were next undertaken in the straight channel with transducers located at 4, 6, 8 and 10 m from the generator, and with uniform water depths of 10, 20 and 30 cm, respectively. Duplicate runs were made at two generator-stroke settings, giving nearly identical wave trains, one of which was approximately twice the amplitude of the other, in order to detect any possible amplitude dependency.

A second series of records was obtained for similar wave trains incident upon beaches of uniform slopes: $s = \frac{1}{32}, \frac{1}{16}, \frac{1}{8}$. In each experiment the water depth was maintained at 30 cm in the straight channel section ahead of the beach, and

the toe of the beach slope, as well as the first transducer, was located 8 m from the generator. Three more transducers were located over the slope being tested at distances where the water depths were always 15, 5 and 1 cm, respectively. Again, duplicate runs were made at single and double amplitude in each case.

Following the experiments, the original records were taped to a drawing board and smooth envelopes drawn through the extrema of the wave trains, as shown in figure 2, which is a reproduction of a typical record made by digitizing the original recording and obtaining a machine plot on the computer. Next, several ordinates were drawn at convenient frequency intervals,† and the spectral amplitudes read from the intersections of the ordinate lines with the wave envelopes. The amplitudes were then corrected for transducer calibration, and the amplitude ratios between the 8 m transducer and the other three stations computed for each frequency.

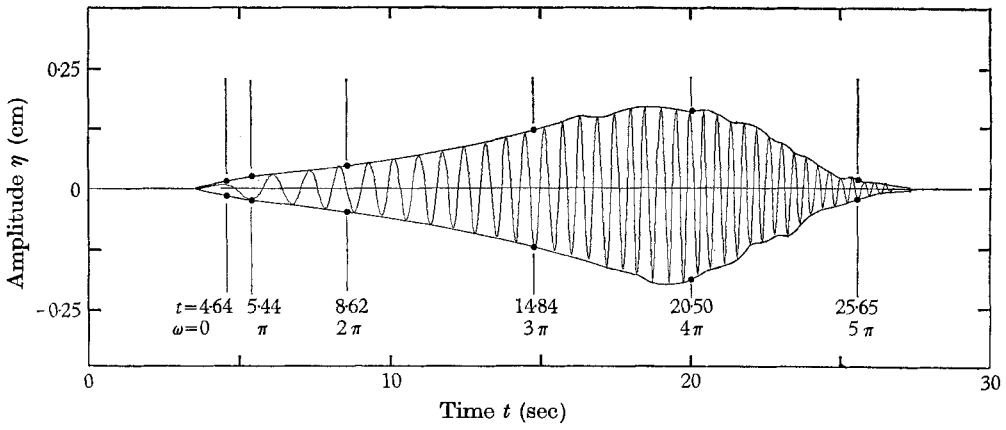

FIGURE 2. Typical wave train recorded 8 m from generator, showing method of determining wave envelope (spectral) amplitudes.

5. Results

The time change in amplitude resulting from increasing surface dissipation for waves propagating down a uniform channel is shown in figure 3 (but only schematically) where the observed amplitude ratio $\eta_{x=8m}/\eta_{x=4m}$ is given as a function of frequency at 20 min intervals, starting with freshly filtered tap water. The solid curves were computed from (6) for an uncontaminated ($\cosh^2$ term unity) and fully contaminated surface.‡ Under the conditions of this experiment, com-

† In the case of a uniform channel, the arrival time of any frequency at a distance x from the generator is

$$t_\omega = x/U(\omega). \tag{8}$$

For a channel terminating at $x = x_0$ in a slope s, the arrival time is

$$t_\omega = \frac{x_0}{U_0} + \int_{x_0}^{x} \frac{dx}{U} = \frac{x_0}{U_0} + \frac{2(k_0 h_0 - kh)}{\omega s}. \tag{9}$$

The integration of (9) is carried out by the same method as that leading to equation (A 7) This simple result seems not to have been given before.

‡ In all cases, the viscosity used was that appropriate to the temperature at the time of the test.

plete contamination occurred within an hour, and the observational data fully confirm the theory for both extreme conditions. At the highest frequency ($\omega = 5\pi$), surface dissipation accounts for 80 % of the total effect.

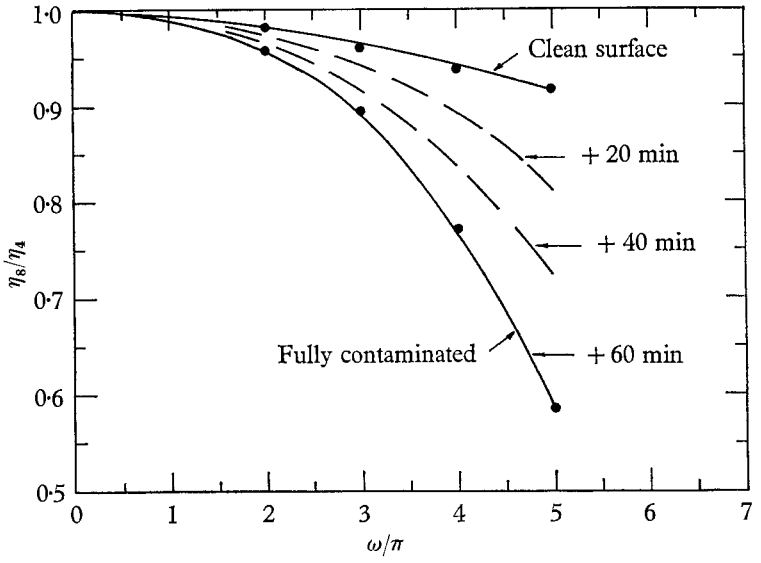

FIGURE 3. Time change of boundary dissipation with increasing surface contamination. Curves were computed from equation (6).

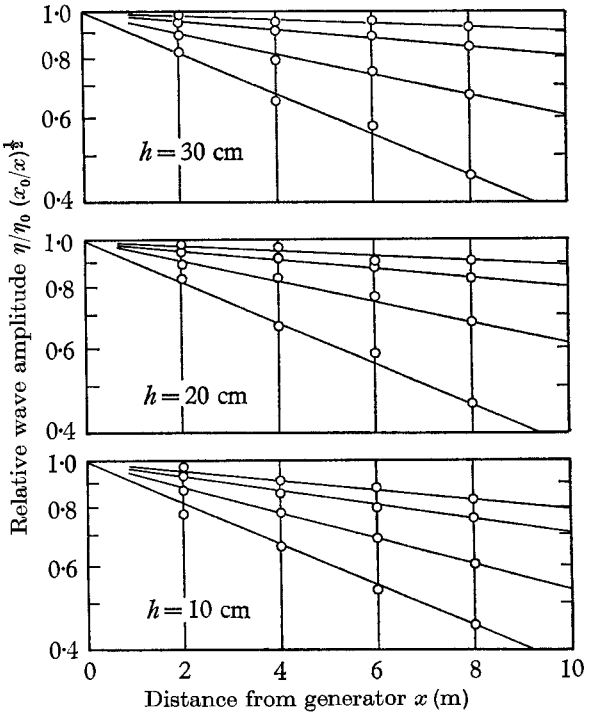

FIGURE 4. Wave dissipation in a uniform channel as a function of channel length, for fully contaminated surface. Frequencies in descending order are $\omega = \pi$, 2π, 3π 4π.

Figure 4 compares the computed and observed dissipation as a function of travel distance for four frequencies and three (uniform) water depths, for a fully-contaminated surface. In these figures the amplitude ratios have been divided by the square-root of their respective distance ratios to normalize them to a common origin and to show the exponential character of the dissipation corrections. Again, the data appear to confirm adequately the theory for uniform depth.

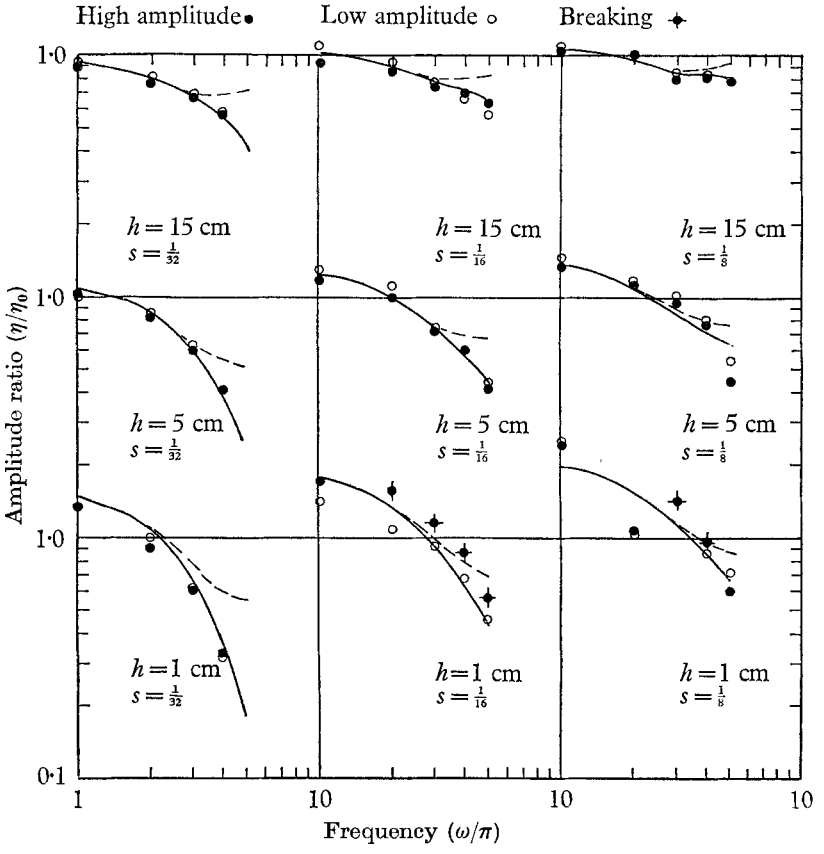

FIGURE 5. Wave dissipation over a sloping beach for fully-contaminated surface. Dashed (uncontaminated) and solid (contaminated) curves were computed from equation (7).

The results of the dissipation experiments over uniform slopes are shown in the nine pairs of curves of figure 5, where the amplitude ratios are referred to the reference amplitudes at the toe of the slope, for three slopes and three water depths. The dashed and solid curves give the theoretical dissipation computed from equation (7) for an uncontaminated and fully-contaminated surface, respectively. Because of their complexity, and also because the local wave-number k is a root of the implicit relation $\omega^2 = gk \tanh kh$ which must be found by iteration for each step in the indicated summations, equation (7) was programmed for computer calculation. With the smallest slope ($s = \frac{1}{32}$), the data are still in good agreement with linear theory but the agreement becomes progressively poorer with decreasing depth and increasing slope. Even in the

worst case ($h = 1$ cm, $s = \frac{1}{8}$), however, and with incipient breaking of the highest waves, the maximum error is about 50 %.

The result is quite surprising in view of the extent by which some of the experimental conditions violated the inequalities assumed in the theoretical development given above. These inequalities, together with their appropriate values computed from the observed data, are given in table 1. None of the data points satisfy all three conditions, and in some cases where the data agree very well with the computed curves the linearity assumption is exceeded by almost two orders of magnitude.

Slope s	...	$\frac{1}{32}$			$\frac{1}{16}$			$\frac{1}{8}$	
Depth h (cm)	15	5	1	15	5	1	15	5	1
				(*a*) Linearity assumption: $\eta/\sigma^2 h \ll 1$					
ω/π									
1	0·008	0·077	2·94	0·011	0·119	5·49	0·007	0·081	0·471
2	0·004	0·040	1·02	0·004	0·056	2·14	0·004	0·032	0·947
3	0·003	0·026	0·681	0·003	0·031	1·29	0·002	0·036	1·43
4	0·001	0·014	0·316	0·002	0·025	0·655	0·002	0·028	1·03
5	†	†	†	0·000	0·001	0·069	0·000	0·003	0·149
				(*b*) Small-amplitude assumption: $\eta/h \ll 1$					
1	0·001	0·004	0·030	0·002	0·006	0·056	0·001	0·004	0·048
2	0·003	0·009	0·042	0·003	0·012	0·088	0·003	0·007	0·039
3	0·006	0·014	0·064	0·006	0·016	0·121	0·005	0·019	0·134
4	0·006	0·015	0·054	0·012	0·027	0·112	0·010	0·030	0·176
5	†	†	†	0·004	0·003	0·019	0·005	0·006	0·041
				(*c*) Geometric-optics assumption: $s/\sigma \ll 1$					
1	0·079	0·138	0·310	0·157	0·275	0·619	0·313	0·551	1·24
2	0·036	0·067	0·154	0·073	0·136	0·308	0·145	0·269	0·616
3	0·021	0·043	0·103	0·042	0·086	0·204	0·083	0·172	0·408
4	0·013	0·030	0·076	0·025	0·060	0·151	0·051	0·121	0·303
5	†	†	†	0·017	0·044	0·119	0·033	0·088	0·239

† Amplitudes too small to be resolved.

TABLE 1. Conditions for applicability of theory ($\sigma \equiv kh$).

6. Discussion

The results cited probably represent a good example of what one can learn from a fairly precise experiment, and indicate that linear theory can often be extended well beyond its assumed range of validity. Clearly, in the shallowest water, many of the waves were markedly asymmetric and on the verge of breaking, but the widest departures from the predicted values occurred because of reflexions from the steeper slopes, as manifested by modulation beats with the incident wave system. What is more remarkable is that a dispersive wave system can apparently be treated as the Fourier superposition of its harmonic components, even in a markedly non-linear régime.

Consideration of either figure 5 or equations (6) and (7) shows that all dissipative effects become negligibly small at frequencies substantially lower than postulated to avoid capillary effects. Thus these results will be of practical concern only over the rather limited range of frequencies considered above.

This work was supported by the Office of Naval Research and the Defense Atomic Support Agency under contracts Nonr 2216(16) and Nonr 2216(20). I am indebted to Prof. G. Backus, Institute of Geophysics and Planetary Physics, University of California, for the suggestion that the surface effect might be important.

Appendix 1. The surface damping coefficient in water of finite depth

Assuming the surface to be horizontally immobilized, but with the wave particle velocity u_0 beneath the boundary layer to be the same as if the contaminating film were absent, the modulus of decay τ is given by the ratio of the average dissipation to the mean total energy of the motion (Landau & Lifshitz 1959, p. 244)

$$\frac{1}{\tau} = \frac{\rho|u_0|^2(\nu\omega/8)^{\frac{1}{2}}}{\rho|u_0|^2/2k} = k\omega^2(\nu/2\omega)^{\frac{1}{2}}. \tag{A 1}$$

Recalling that the modulus of decay for progressive waves is related to the damping coefficient by $\Delta_s = 1/\tau U$ and that, for linear waves in water of finite depth $\omega^2 = gk\tanh kh$ and $U = (\omega/2k)(1+2k/\sinh 2kh)$, we obtain the formula (4) of §2 from (A 1) above directly.

Although a corresponding result can be obtained for a clean water surface, the surface dissipation in the frequency range considered is completely negligible.

Appendix 2. Amplitude change over a sloping bottom

We start with the integral form of (6), from §2,

$$\frac{\eta}{\eta_0} = A[h(\omega)]\exp\left[-\frac{2}{b}\left(\frac{\nu}{2\omega}\right)^{\frac{1}{2}}\int_{x_0}^{x}\left(\frac{b\cosh^2 kh+\sinh 2kh}{2kh+\sinh 2kh}\right)k\,dx\right], \tag{A 2}$$

where A is the shoaling coefficient. Let the slope s be related to depth by

$$h = h_0 - s(x-x_0)$$

such that $dh = -s\,dx$. Then the integral in (A 2) becomes

$$\frac{1}{s}\int_{h_0}^{h}\left(\frac{bk\cosh^2 kh+\sinh 2kh}{2kh+\sinh 2kh}\right)k\,dh.$$

Integration is simplified by the change of variable $\sigma = kh$,

$$\frac{1}{s}\int_{h_0}^{h}\left(\frac{(b\sigma/h)\cosh^2\sigma+\sinh 2\sigma}{2\sigma+\sinh 2\sigma}\right)\frac{\sigma}{h}\,dh, \tag{A 3}$$

where σ and ω are related by

$$\omega^2 h/g = \sigma\tanh\sigma. \tag{A 4}$$

Differentiating (A 4) and rearranging terms, we get

$$(\sigma/h)\,dh = (2\sigma + \sinh 2\sigma)\,(\sinh 2\sigma)^{-1}\,d\sigma. \tag{A 5}$$

Substitution of (A 5) in (A 3) gives

$$\frac{1}{s}\int_{\sigma_0}^{\sigma}\left(\frac{b\omega^2}{2g}\coth^2\sigma + 1\right)d\sigma, \tag{A 6}$$

which integrates to

$$\frac{1}{s}\left[\left(1+\frac{b\omega^2}{2g}\right)(\sigma-\sigma_0) - \frac{b\omega^2}{2g}\,(\coth\sigma - \coth\sigma_0)\right].$$

If we return to the original variables and use (A 4), (A 2) can now be written

$$\frac{\eta}{\eta_0} = A[h(x)]\exp\left\{\frac{1}{s}\left(\frac{\nu}{2\omega}\right)^{\frac{1}{2}}\left[\left(\frac{2}{b}+\frac{\omega^2}{g}\right)(kh - k_0h_0) - 2(k-k_0)\right]\right\}, \tag{A 7}$$

which is the same as (7), § 2.

REFERENCES

DAVIES, J. T. & VOSE, R. W. 1965 *Proc. Roy. Soc.* A, **286**, 218.

DORRESTEIN, R. 1951 *Kon. Ned. Akad. Wet.* B, **54**, 260.

EAGLESON, P. S. 1959 *Mass Inst. Tech. Hydrodynamics Lab. Tech. Rep.* no. 32.

GROSCH, C. E. 1962 *Phys. Fluids*, **5**, 1163.

HUNT, J. N. 1952 *La Houille Blanche*, **7**, 836.

HUNT, J. N. 1963 *Phys. Fluids*, **7**, 156.

KEULEGAN, G. 1959 *J. Fluid Mech.* **6**, 33.

KRANZER, H. C. & KELLER, J. B. 1959 *J. Appl. Phys.* **30**, 398.

LAMB, H. 1945 *Hydrodynamics*. New York: Dover.

LANDAU, L. D. & LIFSHITZ, E. M. 1959 *Fluid Mechanics*, Ch. 6. Reading, Mass.: Addison-Wesley.

VAN DORN, W. G. 1964 *J. Mar. Res.* **22**, 123.